Journal of Mathematical Modeling
Vol. 10, No. 4, 2022, pp. 417-435. Research Article

JMM

A mathematical model to simulate the drug release pattern from drug-eluting stents with biostable polymeric bulk and hydrophobic incorporated drug

Hadiseh Kamalgharibi[†], Akbar Hashemi Borzabadi[†,‡,*], Omid Solaymani Fard[†,§], Atefeh Solouk Mofrad [◇], Mahdi Shafieian[◇]

[†]*School of Mathematics and Computer Science, Damghan University, Damghan, Iran*
[‡]*Department of Applied Mathematics, University of Science and Technology of Mazandaran, Iran*
[§]*Faculty of Mathematical Science, Ferdowsi University, Mashhad, Iran*
[◇]*Department of Biomedical Engineering, Amirkabir University of Technology, Tehran, Iran*
Email(s): Hadiskmly@gmail.com, borzabadi@mazust.ac.ir, omidsfard@gmail.com, atefeh.solouk@gmail.com, shafieian@aut.ac.ir

Abstract. DES, or drug-eluting stents, have the advantage of reducing restenosis rates relative to bare-metal stents. Modeling and simulation can be used to improve device performance. In this study, a general mathematical model for releasing a hydrophobic drug from a drug-eluting stent, DES, with a biostable coating is modeled. Most mathematical models allow the drug in the polymer to be released freely. This is suitable when the initial concentration of the drug in the polymer is less than the solubility, in which case the dissolution of the drug can be considered instantaneously. On the other hand, matrix devices can be loaded above solubility to provide zero-order release. to this end, we have equipped a model with a function that determines how the dissolution processes change with the dispersed phase discharge. The general model is analyzed with some limitations, and it is reduced to a new model that is consistent with previous studies. We examine the effects of initial drug loading and dissolution rate constant in numerically solving one of the new models, which is novel in DESs.

Keywords: Mathematical model, drug eluting stent, biostable polymer, dissolution, diffusion.
AMS Subject Classification 2010: 34A34, 65L05.

1 Introduction

Novel drug delivery systems, also known as Controlled drug delivery systems, will be able to control and determine the rate, time, and place of drug release. Generally, these devices fall into two categories:

*Corresponding author.
Received: 25 November 2021 / Revised: 4 February 2022/ Accepted: 4 February 2022
DOI: 10.22124/jmm.2022.21157.1850

matrix devices and membrane controlled devices (or reservoir systems) [17]. One of the ways to deliver drugs is to use drug-eluting stents (DESs). Unlike classical metal stents, polymer-coated stents show high plasticity and facilitate the placement of prostheses at the implantation site. The polymeric coating is, therefore, a suitable matrix for the controlled immobilization and release of antiproliferative drugs. Polymer layers on the stent surface have the following roles: (1) inhibiting the drug from being washed off from the stent surface, (2) providing a suitable scaffold for drug loading, (3) providing an engineered control over the drug release, and (4) providing a satisfactory platform for biocompatibility. A drug-eluting stent is less likely to re-block arteries, so it helps eliminate the need to repeat angioplasty procedures, which carry complications like heart attacks and strokes [29, 37]. Slowly releasing the drug, interrupts the smooth muscle cell cycle and thus their proliferation. As a result, restenosis can be significantly reduced [8]. Mathematical modeling can be used to analyze complex systems quantitatively. Indeed, a mathematical model may be regarded as a language that narrates hypotheses and talks about the implications of those hypotheses. In the early years, the drug release mechanism was poorly understood, but mathematical modeling and experiments have helped researchers identify the dominant mechanisms for drug release in a variety of stents. Mathematics models have the advantage that they permit parameter variation and comparison of release profiles without the need to repeat the experiments once they have been verified. An important benefit of mathematical modeling is its ability to identify the important variables that govern drug release. Additionally, modeling can be useful to understand how drugs are distributed within arterial tissue [6, 20]. Zunino conducted the first mathematical study of drug stents [38] that was too simplistic to predict drug distribution on arterial walls. So far, Several computer simulations and modeling studies have been conducted on drug-eluting stents. A bunch models are presented on polymer coatings according to physical properties, geometry design [13, 27], chemical properties of drug [2, 35], stent coating such as non-erodible polymer [16], biodegradable and erodible coatings [5, 31] in one, two and three dimensions [8, 9, 15, 16, 20]. Modeling the release of drugs from arterial stents is only one part of the story. Simulation of drug distribution in arterial walls is another aspect of modeling. Models involving advection-diffusionreaction equation [10] and drug binding in arterial tissue using linear and non-linear reaction terms [25, 26] are developed. The convective and diffusive transports of drug in the arterial wall [34] has been assessed for both hydrophilic and hydrophobic drugs. A stent and arterial wall are, of course, a coupled system (or stents and arterial walls are, of course, a coupled system). Thus, to accurately represent the in vivo situation, we must take into account the interaction between the stent and the tissue. McGinty et al. [20, 21] presented one of the first stent/tissue models that accounted for convection, diffusion, and uptake into SMCs within porous media. The drug release profile is one of the most important aspects of the performance of DESs. Due to the expense and time associated with in vivo experiments, stent manufacturers routinely test the release of drugs from their stents in an in vitro environment [21]. Matrix devices, such as polymer coating stents, can be loaded above their solubility to cover zero-order release. Two distinct physical processes occur in this case: diffusion of the dissolved drugs and dispersion of the dispersed molecules. In this case, some researches in 2D or 3D considering some special limitations have only been presented theoretically, such as high dissolution rate [37] and in other studies, release governed by a diffusion-dissolution equation involving a linear first-order reaction in biostable polymer has been considered or a non-linear dissolution term based on a reformulation of the empirical Noyes-Whitney equation for polymers which included surface erosion with finite dissolution rate has been discussed [11, 22].

In light of all the above, the present research aims to develop a general mathematical model for biostable stent coatings loaded with hydrophobic drugs which are equipped with a suitable function to

determine how the dissolution process changes by depleting the dispersed phase. As stated in [19,30,37], here we address drug distribution in the arterial wall with reversible binding.

The outline of this paper is described as follows. In Section 2 we introduce the general model that we introduced above, and in Section 3, we discuss some limitations of the model. We simulated one of the reduced models from a general model that has been never simulated before and because of the nonlinear equations and complicated geometry, a numerical method is presented to solve problems in Section 4 and at the end, results are discussed and the impact of a few parameters is investigated and conclusions are drawn.

2 Mathematical model

In this section, a drug delivery system is considered that takes form a stent with a non-swelling and biostable coating that delivers a hydrophobic drug. Drug transport by diffusion has been identified as the dominant mechanism in the coating and arterial wall and, convective drug transport is not considered in the wall [3]. The concentration of drug dissolved in the coating of the stent and the arterial wall is denoted by C_p and C_w, respectively. Since the initial concentration of a drug may be greater than the solubility of a drug, the excess of a drug must be dissolved before diffuse into the arterial wall. So dissolution process is modeled based on Noyes-Whitney as

$$\frac{\partial C}{\partial t} \sim (C_s - C)\Gamma(C_u), \tag{1}$$

so that $\Gamma(C_u)$ determines how the dissolution processes change as the dispersed phase. Here the undissolved drug in coating is denoted by C_u, that $C_u = C_L - C_s$, where C_L is the initial loading of drug and C_s is the solubility of drug. If there is no solid drug, then $C_u = 0$ and $\Gamma(C_u) = 0$. Note that it is clear that $\sup\Gamma(C_u) = 1$ [17]. According to the above, the governing equations of diffusion-dissolution process in coating can be presented as

$$\frac{\partial C_p}{\partial t} = D_p \bigtriangledown_X^2 C_p + k_{ds}(C_s - C_p)\Gamma(C_u), \;\; X \in \Omega_c, \tag{2}$$

$$\frac{\partial C_u}{\partial t} = -k_{ds}(C_s - C_p)\Gamma(C_u), \;\; X \in \Omega_c, \tag{3}$$

where D_p is the coating drug diffusivity and k_{ds} is the dissolution rate constant, Ω_c represent the area of polymer coating.

On the other hand, the free drug that transports from the polymer coating into the arterial wall has been modeled with reversible binding that is described as a first-order reversible reaction $C_w + S_0 \Longleftrightarrow B$ with association (binding) and dissociation (unbinding) reaction rates k_a and k_d, respectively:

$$\frac{\partial C_w}{\partial t} = D_w \bigtriangledown_X^2 C_w - k_a(S_0 - B)C_w + k_d B, \;\; X \in \Omega_w, \tag{4}$$

$$\frac{\partial B}{\partial t} = k_a(S_0 - B)C_w - k_d B, \;\; X \in \Omega_w, \tag{5}$$

where Ω_w specifies the area of arterial wall and D_w is drug diffusivity. Here, S_0 is the local density of the binding site, and C_w is the free drug that reacting into bound drug B. Although we shall not update a

new model for the distribution of drugs in the arterial wall here, we include a model as stated in [19, 30, 37], with reversible binding for completeness. Note that for hydrophobic drugs such as Sirolimus and Paclitaxel, the velocity vector for tissue domain is set zero and neglected drug flux at the lumenvascular wall and the lumencoating interfaces is justified.

Also zero flux in coatingstrut interface is considered [35, 37]. If the polymer coating is a reservoir device, then

$$C = \alpha C_s, \tag{6}$$

in coatingstrut interface, where α is the membrane/reservoir partition coefficients and C_s is the concentration of the saturated reservoir of drug [17].

In the arterial wall, due to symmetry boundary conditions, we have zero flux to the interfaces rightleft wall boundaries [37]. At the interfaces of perivascular-arterial wall, the flux is represented as following

$$J_{pw} = \frac{1}{R_{pw}}(\frac{C_w}{k_{pw}} - C_{pv}), \tag{7}$$

where R_{pw} is the mass transfer resistance, C_w is the concentration of drug on the arteriall wall of interface, k_{pw} is the partition coefficient and C_{pv} is the concentration of drug on perivascular that is assumed zero [14, 37]. And finally, continuous flux condition at the wall-coating interface is [35]

$$C_p = k_{cw} C_w, \tag{8}$$

$$flux\,|_{\Omega_w} = flux\,|_{\Omega_c}\,. \tag{9}$$

It is assumed that the drug loaded uniformly and the initial conditions are given by

$$C_p(X,0) = C_s, \quad C_u(X,0) = C_L - C_s, \tag{10}$$

$$C_w(X,0) = 0, \quad B(X,0) = 0. \tag{11}$$

2.1 Non-dimensionalisation

The general governing equations may be nondimensionalized by taking

$$\overline{C_i} = \frac{C_i}{C_s},\ i = p,w, \qquad \overline{B} = \frac{B}{s_0}, \qquad \overline{C_u} = \frac{C_u}{C_s}, \tag{12}$$

$$\overline{X} = \frac{X}{\delta} \qquad (X) \in \Omega_c, \quad \overline{X} = \frac{X}{L_{x_i}} \qquad X = (x_1,..,x_n) \in \Omega_c, n = 1,2,3, \tag{13}$$

where δ is the polymer coating thickness and L_{x_i} is the arterial wall length with $\Gamma(C_u) = \overline{\Gamma}(\overline{C_u})$. Now by dropping the overbars, the dimensionless governing equations may be written as fallows

$$\begin{aligned}
\frac{\partial C_p}{\partial t_1} &= \bigtriangledown_X^2 C + k_c(1-C_p)\Gamma(C_u),\ X \in \Omega_c,\\
\frac{\partial C_u}{\partial t_1} &= -k_c(1-C_p)\Gamma(C_u),\ \ X \in \Omega_c,\\
\frac{\partial C_w}{\partial t_2} &= \nabla((A_{11},.,A_{ii})\cdot\nabla C_w) - A_2(1-B)C_w + A_3 B, i = 2,3\ X \in \Omega_w, \qquad (14)\\
\frac{\partial B}{\partial t_3} &= A_4(1-B)C_w - B,\ X \in \Omega_w, \qquad (15)
\end{aligned}$$

where

$$k_c = k_{ds}\frac{\alpha^2}{D_p},\ A_{11}=1,\ A_{ii}=\frac{4D_w(i)L_{x_1}^2}{D_w(1)L_{x_i}^2},\ A_2=\frac{L_{x_1}^2 s_0 k_a}{D_w(1)},\ A_3=\frac{S_0 k_d}{C_0},$$
$$A_4 = \frac{A_2}{A_3},\ t_1=\frac{D_p}{\delta^2}t,\ t_2=\frac{D_w(1)}{L_{x_1}^2}t,\ t_3=\frac{1}{k_d}t.$$

In this paper, we have presented a general model of drug release from a biostable polymer coating. In the following section, some limitations based on physical or chemical processes are considered whereby the governing equations are analyzed.

3 Analysis of general model

In general, the equations are in one, two, or three-dimensional. To simplify the analysis, we continue studies with a cross-sectional model of a coronary artery that a stent with eight struts is implanted it and each strut is in square form as Fig. 1 [1,5]. So in the following, the equations are presented and discussed

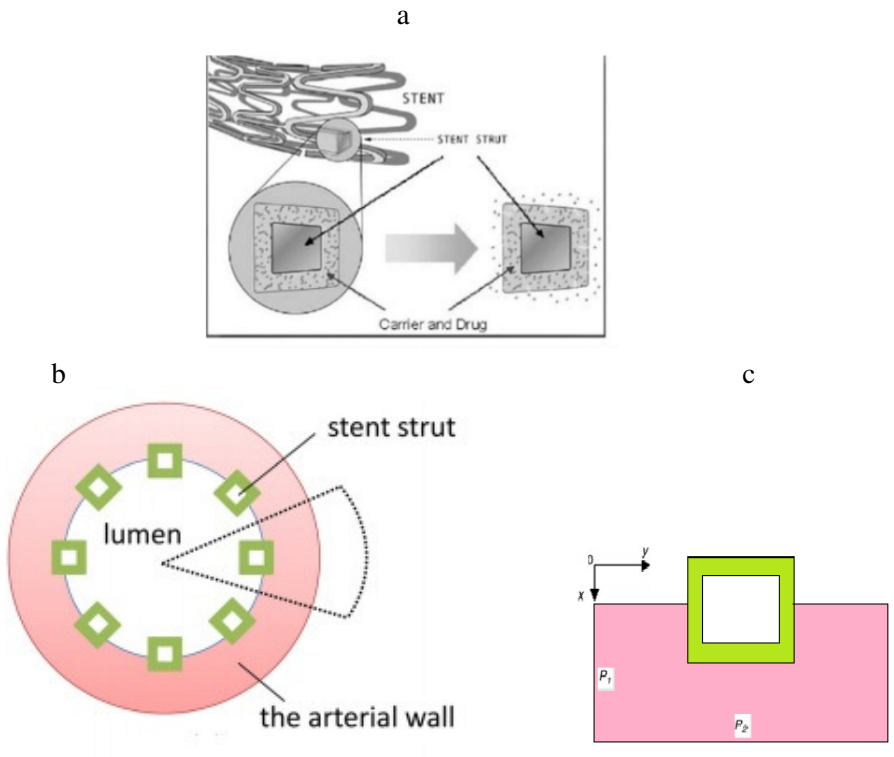

Figure 1: (a) Drug-eluting stent components [1]. (b) Cross-sectional view of an implanted stent in a coronary artery [5]. (c) Schematic of a single strut section that considered as a rectangular arterial wall domain due to small thickness of the coronary artery wall compared to the diameter of the lumen.

in two dimensional.

3.1 Governing equations and boundary conditions in low drug loading

Consider that drug loading is equal or less than the solubility drug, i.e, $C_u = 0$ and $\Gamma(0) = 0$. Therefore, the governing equations are

$$\frac{\partial C_p}{\partial t_1} = \frac{\partial^2 C_p}{\partial x^2} + \frac{\partial^2 C_p}{\partial y^2}, \qquad (x,y) \in \Omega_c, \tag{16}$$

$$\frac{\partial C_w}{\partial t_2} = \frac{\partial^2 C_w}{\partial x^2} + A_{22}\frac{\partial^2 C_w}{\partial y^2} - A_2(1-B)C_w + A_3 B, \quad (x,y) \in \Omega_w, \tag{17}$$

$$\frac{\partial B}{\partial t_3} = A_4(1-B)C_w - B, \qquad (x,y) \in \Omega_w, \tag{18}$$

that refers to mathematical modeling in [37] with referencing boundary conditions.

3.2 Governing equations and boundary conditions in high drug loading

Here we consider that the initial loading of drug is higher than the solubility and the rate of dissolution is large. Also, drug disappears due to diffusion, or interconversion is quickly replaced by drug coming into solution [17, 21]. So the coating may divide up to two distinct regions Ω_1 and Ω_2 which is separated by a moving boundary $s(t) = (s_1, s_2)$ that s_1 and s_2 are the moving boundary in x and y, respectively. The equation in coating changes to a moving boundary problem as following

$$\begin{aligned}
\frac{\partial C_u}{\partial t} &= 0, \quad C_p(X) = constant, && (x,y) \in \Omega_1,\\
\frac{\partial C_p}{\partial t} &= \frac{\partial^2 C_p}{\partial x^2} + \frac{\partial^2 C_p}{\partial y^2}, \quad C_u = 0, && (x,y) \in \Omega_2,\\
\frac{\partial C_w}{\partial t_2} &= \frac{\partial^2 C_w}{\partial x^2} + A_{22}\frac{\partial^2 C_w}{\partial y^2} - A_2(1-B)C_w + A_3 B, && (x,y) \in \Omega_w,\\
\frac{\partial B}{\partial t_3} &= A_4(1-B)C_w - B, && (x,y) \in \Omega_w.
\end{aligned}$$

In this case at $s(t)$ the Stephan conditions are as follow

$$C(s^+(t),t) = C_s, \quad -D\frac{\partial C_p}{\partial x} = \frac{\partial s_1}{\partial t}, \quad -D\frac{\partial C_p}{\partial y} = \frac{\partial s_2}{\partial t}, \tag{19}$$

and at $t = 0$ the $s(t)$ is located at coating-wall interface. All the remind boundary conditions is as said as general model in Section 2

On the other hand, if the rate of dissolution is finite, then dissolution-diffusion equations in the coating are as follows

$$\begin{aligned}
\frac{\partial C_p}{\partial t_1} &= \frac{\partial^2 C_p}{\partial x^2} + \frac{\partial^2 C_p}{\partial y^2} + k_c(1-C_p)\Gamma(C_u), && (x,y) \in \Omega_c,\\
\frac{\partial C_u}{\partial t_1} &= -k_c(1-C_p)\Gamma(C_u), && (x,y) \in \Omega_c,
\end{aligned}$$

with coupled two equations in arterial wall (14)-(15). The initial conditions are as follows,

$$C_p(0,x,y) = 1, \quad (x,y) \in \Omega_c, \tag{20}$$

$$C_u(0,x,y) = \frac{C_L}{C_s} - 1, \quad (x,y) \in \Omega_c, \tag{21}$$

$$C_w(0,x,y) = 0, \quad (x,y) \in \Omega_w, \tag{22}$$

and the boundary conditions are as mentioned previously in Section 2.

4 Numerical simulation

In this section, we aim to simulate the governing model in limitations with high drug loading and finite dissolution rate. Note that a simple dissolution function would be introduced by a step function that is applicable to saturated- reservoir system. To this end, for the duration of application, if $C_u > 0$ then $\Gamma(C_u) = 1$ and if there is no dispersed drug, then $\Gamma(C_u) = 0$. Here we considered a matrix device with the above limitation that $\Gamma(C_u)$ is adopted with a convenient smoothed approximation to a step function that is

$$\Gamma(C_u) = \tanh C_u. \tag{23}$$

So in special case, high drug loading and finite dissolution rate, the following equations are derived, free drug in the polymer coating

$$\frac{\partial C_p}{\partial t} = D_{p1}\frac{\partial^2 C_p}{\partial x^2} + D_{p2}\frac{\partial^2 C_p}{\partial y^2} + K_{dc}(1-C_p)\tanh C_u, \quad x,y \in \Omega_p \tag{24}$$

$$\frac{\partial C_u}{\partial t} = -K_{dc}(1-C_p)\tanh(C_u), \quad x,y \in \Omega_p, \tag{25}$$

and free and bound drug in the arterial wall

$$\frac{\partial C_w}{\partial t} = D_{w1}\frac{\partial^2 C_w}{\partial x^2} + D_{w2}\frac{\partial^2 C_w}{\partial y^2} - k_a(S_0 - B)C_w + k_d B, \ x,y \in \Omega_w, \tag{26}$$

$$\frac{\partial B}{\partial t} = k_a(S_0 - B)C_w - k_d B, \ (x,y) \in \Omega_w. \tag{27}$$

with the boundary and initial conditions stated in Section 2.

The model with fixed boundary is simulated with an explicit finite volume method that is outlined by [24]. To this end, let Δ_x and Δ_y be the special steps, i, j be indices for x, y coordinates, Δ_t denotes the time step and n be the time index. To illustrate how the numerical scheme was developed, let us start by integrating (24) over the control volume of size Δ_x and Δ_y centred at (x,y), as follows:

$$\int_{y-\Delta_y/2}^{y+\Delta_y/2}\int_{x-\Delta_x/2}^{x+\Delta_x/2}\frac{\partial C_p}{\partial t}dx\,dy = J_x|(x-\Delta_x/2,y)\Delta_y - J_x|(x+\Delta_x/2,y)\Delta_y + J_y|(y-\Delta_y/2,x)\Delta_x$$
$$-J_y|(y+\Delta_y/2,x)\Delta_x + \int_{y-\Delta_y/2}^{y+\Delta_y/2}\int_{x-\Delta_x/2}^{x+\Delta_x/2} k_{dc}(1-C_p)\tanh(C_u)dx\,dy,$$

where J_x and J_y are influx/out flux in their directions. In the following, by using forward-difference approximation for the time derivative, we get

$$\frac{\tilde{C}^{n+1}_{p^{i,j}} - \tilde{C}^{n}_{p} i,j}{\Delta_t} = \frac{1}{\Delta_x}(J_x|^n_{i-\frac{\Delta_x}{2},j} - J_x|^n_{i+\frac{\Delta_x}{2},j}) + \frac{1}{\Delta_y}(J_y|^n_{i,j-\frac{\Delta_y}{2}} - J_y|^n_{i,j+\frac{\Delta_y}{2}}) + k_c(C_s - (\tilde{C}^n_{p^{i,j}}))(\tilde{\Gamma}(C^n_{u^{i,j}})), \quad (28)$$

where

$$J_x|^n_{i+\frac{\Delta_x}{2},j} = -D_{p1}\frac{\tilde{C}^n_{p^{i+\Delta_x,j}} - \tilde{C}^n_{p^{i,j}}}{\Delta_x}, \quad (29)$$

and $\tilde{C}_p$ and $\Gamma(\tilde{C}_U)$ are the average values of C_P and $\Gamma(C_U)$ on cell centroid (i,j) respectively. For example, the $\tilde{C}_p$ is calculated by

$$\tilde{C}_{p^{i,j}} = \frac{1}{\Delta_x \Delta_y}\int_{i-\frac{\Delta_x}{2},j}^{i+\frac{\Delta_x}{2},j}\int_{i,j-\frac{\Delta_y}{2}}^{i,j+\frac{\Delta_y}{2}} C_P \; dxdy.$$

After spatial discretization, the discretized equations are solved numerically. The computational code has been successfully programmed using MATLAB R2018a on a personal computer.

4.1 Convergence and stability

In this section, the convergence and stability conditions of the numerical method on the polymer coating system is investigated, and due to the similarity and repetition of the proof on the arterial wall and because of the length the proof, we establish the convergence and stability just for (24)-(25), although the convergence and stability for arterial wall have been discussed on [37] .

Theorem 1. *Let C_p and C_u be the exact solution of (24)-(25) which have continuous derivatives $\frac{\partial^2 C_p}{\partial t^2}$, $\frac{\partial^4 C_p}{\partial x^4}$, $\frac{\partial^4 C_p}{\partial y^4}$, $\frac{\partial^2 C_u}{\partial t^2}$ in $\Omega_p \times [0,T]$, if $(D_{p1}(\frac{\Delta_t}{\Delta_x^2}) + D_{p2}(\frac{\Delta_t}{\Delta_y^2})) \leq \frac{1}{2}$, then the approximate solution converges to the exact solution as $\Delta_t \to 0$, $\Delta_x \to 0$ and $\Delta_y \to 0$*

Proof. Denote the exact solution of the equation (28) by C_p and the approximate solution by c_p. Then $e = c_p - C_p$. At the mesh points, let

$$C^k_{p^{i,j}} - e^k_{i,j} = C^k_{p^{i,j}}. \quad (30)$$

Without loss of generality, we assume that $\Delta_x = \Delta_y = h$. Since $\alpha + \beta \leq \frac{1}{2}$, rearranging the terms of (28) and taking magnitudes of both sides leads to

$$|e^{k+1}_{i,j}| \leq (1 - 2\alpha - 2\beta)|e^{k+1}_{i,j}| + \alpha|e^{k+1}_{i,j}| + \alpha|e^{k+1}_{i,j}| + \beta|e^{k+1}_{i,j}| + \beta|e^{k+1}_{i,j}| + M|e^{k+1}_{i,j}|\Delta_t + E_T\Delta_t, \quad (31)$$

where $\alpha = D_1\frac{\Delta_t}{h^2}$, $\beta = D_2\frac{\Delta_t}{h^2}$, M is the maximum magnitude of $(f(C_p)\Gamma(C_u))'$ and E_T is the maximum of local truncation error which may be obtained by the Taylor's series expansion as follows

$$E^K_{T^{i,j}} = (\Delta_t/2)\frac{\partial^2 C_p(x_i, y_j, \tilde{t})}{\partial t^2} - (\Delta_x^2/12)D_1\frac{\partial^4 C_p(\tilde{x}, y_j, t_k)}{\partial x^4} - (\Delta_y^2/12)D_2\frac{\partial^4 C_p(x_i, \tilde{y}, t_k)}{\partial y^4}. \quad (32)$$

So there are M_1, M_2 and M_3 so that

$$|E^K_{T^{i,j}}| \leq M_1\Delta_t + M_2\Delta^2 + M_3\Delta_y^2 \equiv E_T. \quad (33)$$

Let E^k be the maximum value of $|e^k(i,j)|$ for $1 \le i \le n-1$ and $1 \le j \le m-1$. The (31) becomes

$$E^k \le (1+M\Delta_t)^k E^0 + [1+(1+M\Delta_t)+\cdots+(1+M\Delta_t)^{k-1}]E_T\Delta_t. \tag{34}$$

Since $k\Delta_t \le T$, the above scheme becomes

$$E^k \le \frac{(1+M\Delta_t)^{T/\Delta_t}-1}{M}E_T \le \frac{\exp(MT)-1}{M}E_T, \tag{35}$$

when Δ_x , Δ_y and Δ_t tends to zero, $E_T \to 0$ and this proves that c_p converges to C_p. □

To investigate the stability of the approximate solution of nonlinear differential equations (24)-(27), we use matrix method. To this end, the equation (28) is represented in matrix form. If $(n-1)$ are the number of grid points in X-direction and $(m-1)$ the number of points in Y-direction,we can write the solution vector as follows

$$\begin{aligned}\overrightarrow{c_p^k} &= [c^k_{p^1}, c^k_{p^2}, c^k_{p^3}, \ldots, c^k_{p^{(n-1)(m-1)}}]^T \equiv [c^k_{p^{1,1}}, c^k_{p^{1,2}}, c^k_{p^{1,3}}, \ldots, c^k_{p^{(n-1)(m-1)}}, c^k_{p^{2,1}}, c^k_{p^{2,2}}, c^k_{p^{2,3}}, \ldots, c^k_{p^{(n-1)(m-1)}}, \ldots \\ &\ldots, c^k_{p^{n-1,1}}, c^k_{p^{n-1,2}}, c^k_{p^{n-1,3}}, \ldots, c^k_{p^{(n-1)(m-1)}}]^T\end{aligned} \tag{36}$$

and like $\overrightarrow{c_p^k}$, we have $\overrightarrow{c_u^k} = [c^k_{u^1}, c^k_{u^2}, c^k_{u^3}, \ldots, c^k_{u^{(n-1)(m-1)}}]^T$. Therefore, Eq. (28) is expressed in the matrix form as

$$\overrightarrow{c_p^{k+1}} = A\overrightarrow{c_p^k} + \Delta_t \; diag\{f(c^k_{p^1})\Gamma(c^k_{u^1}), f(c^k_{p^2})\Gamma(c^k_{u^3}), \ldots, f(c^k_{p^{(n-1)(m-1)}})\Gamma(c^k_{u^{(n-1)(m-1)}})\} \tag{37}$$

where

$$A = \begin{bmatrix} \gamma_1 & \beta I_{n-1} & 0 & \cdots & 0 & 0 \\ \beta I_{n-1} & \gamma_2 & \beta I_{n-1} & \cdots & 0 & 0 \\ \vdots & \vdots & \vdots & \ddots & \vdots & \vdots \\ 0 & 0 & 0 & \ldots & \gamma_{m-2} & \beta I_{n-1} \\ 0 & 0 & 0 & \ldots & \beta I_{n-1} & \gamma_{m-1} \end{bmatrix}_{((n-1)\times(m-1))^2}.$$

Note that γ_ρ, $\rho = 1, \ldots, m-1$, are tridiagonal matrix that are symmetric and may be different from each other in areas adjacent to the boundary according to boundary conditions. For example for some $c^k_{p^i}$ we have

$$\gamma_\rho = \begin{bmatrix} 1-2\alpha-2\beta & \alpha & 0 & \ldots & 0 & 0 \\ \alpha & 1-2\alpha-2\beta & \alpha & \ldots & 0 & 0 \\ \vdots & \vdots & \vdots & \ddots & \vdots & \vdots \\ 0 & 0 & 0 & \vdots & 1-2\alpha-2\beta & \alpha \\ 0 & 0 & 0 & \vdots & \alpha & 1-2\alpha-2\beta \end{bmatrix}_{(n-1)^2},$$

and there is some rows that γ_ρ is as

$$\gamma_\rho = \begin{bmatrix} 1-\alpha-\beta & \alpha & 0 & \cdots & 0 & 0 \\ \alpha & 1-2\alpha-\beta & \alpha & \cdots & 0 & 0 \\ \vdots & \vdots & \vdots & \ddots & \vdots & \vdots \\ 0 & 0 & 0 & \vdots & 1-2\alpha-\beta & \alpha \\ 0 & 0 & 0 & \vdots & \alpha & 1-\alpha-\beta \end{bmatrix}_{(n-1)^2},$$

and using forward-difference approximation for the time derivative in (25) the following matrix form is derived

$$\overrightarrow{c_u^{k+1}} = I\overrightarrow{c_u^k} + \Delta_t \;\; diag\big\{ -f(c_{p^1}^k)\Gamma(c_{u^1}^k), -f(c_{p^2}^k)\Gamma(c_{u^3}^k), ..., -f(c_{p^{(n-1)(m-1)}}^k)\Gamma(c_{u^{(n-1)(m-1)}}^k)\big\}. \tag{38}$$

Theorem 2. *The system (28) with continuous derivatives of $f(C_P)$ and $\Gamma(C_u)$ is stable if*

$$D_{p1}(\frac{\Delta_t}{\Delta_x^2}) + D_{p2}(\frac{\Delta_t}{\Delta_y^2}) \leq \frac{1}{2}.$$

Proof. By the mean value theorem and (36), the following difference operator may be obtained

$$\begin{aligned}
\overrightarrow{c_p^{k+1}} &= A\overrightarrow{c_p^k} + \Delta_t \;\; diag\big\{f'(c_{p^1}^k)\Gamma(c_{u^1}^k), f'(c_{p^2}^k)\Gamma(c_{u^3}^k), \ldots, f'(c_{p^{(n-1)(m-1)}}^k)\Gamma(c_{u^{(n-1)(m-1)}}^k)\big\}\overrightarrow{c_p^k},\\
\overrightarrow{c_u^{k+1}} &= I\overrightarrow{c_u^k} + \Delta_t \;\; diag\big\{ -f(c_{p^1}^k)\Gamma'(c_{u^1}^k), -f(c_{p^2}^k)\Gamma'(c_{u^3}^k), \ldots, -f(c_{p^{(n-1)(m-1)}}^k)\Gamma'(c_{u^{(n-1)(m-1)}}^k)\big\}\overrightarrow{c_u^k}.
\end{aligned}$$

Let $\overrightarrow{U^k} = [\overrightarrow{c_p^k}, \overrightarrow{c_u^k}]$. So, we have

$$\begin{aligned}
\overrightarrow{U^{k+1}} &= A_U\overrightarrow{U^k} + \Delta_t \;\; diag\big\{f'(c_{p^1}^k)\Gamma(c_{u^1}^k), f'(c_{p^2}^k)\Gamma(c_{u^3}^k), \ldots, f'(c_{p^{(n-1)(m-1)}}^k)\Gamma(c_{u^{(n-1)(m-1)}}^k,\\
&\quad -f(c_{p^1}^k)\Gamma'(c_{u^1}^k), -f(c_{p^2}^k)\Gamma'(c_{u^3}^k), \ldots, -f(c_{p^{(n-1)(m-1)}}^k)\Gamma'(c_{u^{(n-1)(m-1)}}^k)\big\}\overrightarrow{U^k}
\end{aligned}$$

Or $\overrightarrow{U^{k+1}} = \tilde{A}_U\overrightarrow{U^k}$, where

$$\begin{aligned}
\tilde{A}_U &= A_U + \Delta A_k\\
&= A_U + \Delta_t \;\; diag\big\{f'(c_{p^1}^k)\Gamma(c_{u^1}^k), f'(c_{p^2}^k)\Gamma(c_{u^3}^k), \ldots, f'(c_{p^{(n-1)(m-1)}}^k)\Gamma(c_{u^{(n-1)(m-1)}}^k, -f(c_{p^1}^k)\Gamma'(c_{u^1}^k),\\
&\quad -f(c_{p^2}^k)\Gamma'(c_{u^3}^k), \ldots, -f(c_{p^{(n-1)(m-1)}}^k)\Gamma'(c_{u^{(n-1)(m-1)}}^k)\big\}.
\end{aligned}$$

It is clear that $\| A_U \|_\infty = 1$ if $(D_{p1}(\frac{\Delta_t}{\Delta_x^2}) + D_{p2}(\frac{\Delta_t}{\Delta_y^2})) \leq \frac{1}{2}$ that leads to $\rho(A_U) \leq 1$. On the other hand, as mentioned in the previous theorem, $(f(c_p)\Gamma(c_u))'$ is bounded, and it is trivial to verify that $\rho(\Delta A_p) \leq \Delta_t M$. Hence, since A_U and ΔA_p are symmetric, we deduce the inequality

$$\rho(\tilde{A}_U) = \rho(A_U + \Delta A_k) \leq \rho(A_U) + \rho(\Delta A_k) \leq 1 + M\Delta_t. \tag{39}$$

So the von Neumann necessary condition for stability is established. Since $\tilde{A}_U$ is a normal matrix and positive number M is independent of h_1, h_2 and k, the von Neumann condition is sufficient as well as necessary for the stability [18, 28, 32]. Note that for isotropic diffusion, when $\Delta_x = \Delta_y = h$, stability condition is derived as $D(\frac{\Delta_t}{h^2}) \leq \frac{1}{4}$. □

5 Numerical experiments

For the proposed drug release system, first, we compare the figures from numerical computations in high drug loading, $C_0 > C_s$, with low drug loading, $C_0 = C_s$, and following that, the drug loading and the drug dissolution rate constant are investigated for their impact on the drug transport and distribution.

In order to study the diffusion of drug in the coating of strut and delivered drug to the arterial wall, the data set which is indicated in Table 1 is used.

Table 1: Simulated values of the model parameters.

Description	Parameter	Value	Reference
Diameter of the strut	λ	$140\mu m$	[1, 37]
Strut coating thickness	δ	$50\mu m$	[23, 37]
Wall thickness	δ_w	$200\mu m$	[37]
Inter-strut distance	z_d	$0.1cm$	[37]
Coating drug diffusivity	D_p	$0.1\mu m^2 s^{-1}$	[23]
Drug solubilization limit	C_s	$10^{-5}M$	[6]
Free drug diffusion coefficient	D_w	$0.1 - 10\mu m^2 s^{-1}$	[37]
Association rate constant	k_a	$10^{-2}M^{-1}s^{-1}$	[36]
Dissociation rate constant	k_d	$0.01s^{-1}$	[37]
Dissolution rate constants	k_{ds}	$0.05s^{-1}$	[17]
Local density in binding site	S_0	10^{-5} M	[37]

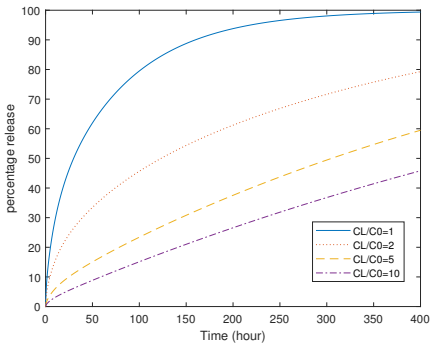

Figure 2: Drug release profile in the stent coating by changing initial drug loading.

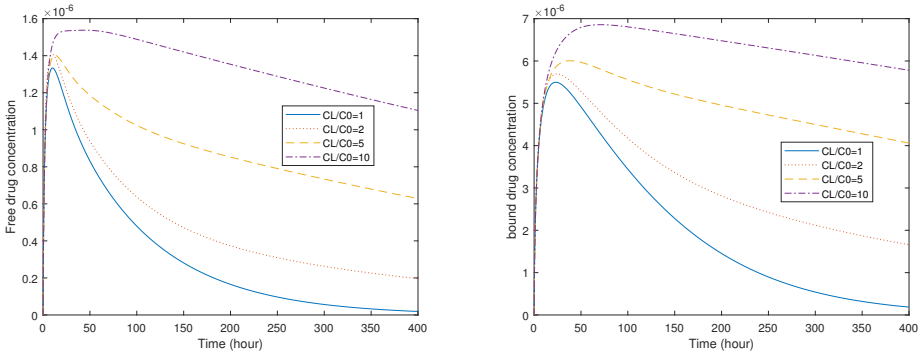

Figure 3: Temporal variation for the spatial average of free and bound drug concentrations in the arterial wall for the different initial drug concentration.

5.1 Impact of high initial loading

As stated in previous studies [4, 22], there may be changes in the rate of release due to initial drug loading. Fig. 2 represents the cumulative percentage of drug released in the stent coating at different C_L so that $(C_L/C_s) = 1, 2, 5, 10$. When the loading initial drug is equal solubility drug, $C_L/C_s = 1$, so there is no dispersed drug and $\tanh C_u = 0$. So the above model changes to equations (16)-(18) and its profile is similar to the investigated in some works [37]. With increasing C_L the profile is in agreement with zero-order profile and the duration of release is prolonged. Fig. 3 plots spatially averaged free-drug and bound-drug concentrations in the arterial wall for different C_L. The simulation shows with increasing the ratio of C_L/C_0 the average concentration of drug in the arterial wall reaches quasi-equilibrium values. The top profile displays the temporal variation of spatially average concentration in $C_L/C_0 = 10$ and has the most equilibrium.

As reported in previous studies, the lack of drug in upper layers far away from the strut in the circumferential direction is potentially linked to the growth of more in-stent restenosis at larger interstrut angle [5, 33]. Fig. 4 represent the impact of initial drug loading in free and bound drug concentration at boundary points p_1 and p_2 which are shown in Fig. 1-(c). In low drug loading, Fig. 4-(a), low quasi-equilibrium drug concentrations are observed at sites p_1 and p_2 while with increasing initial drug loading, quasi-equilibrium levels are reached, Fig. 4-(c) and (d).

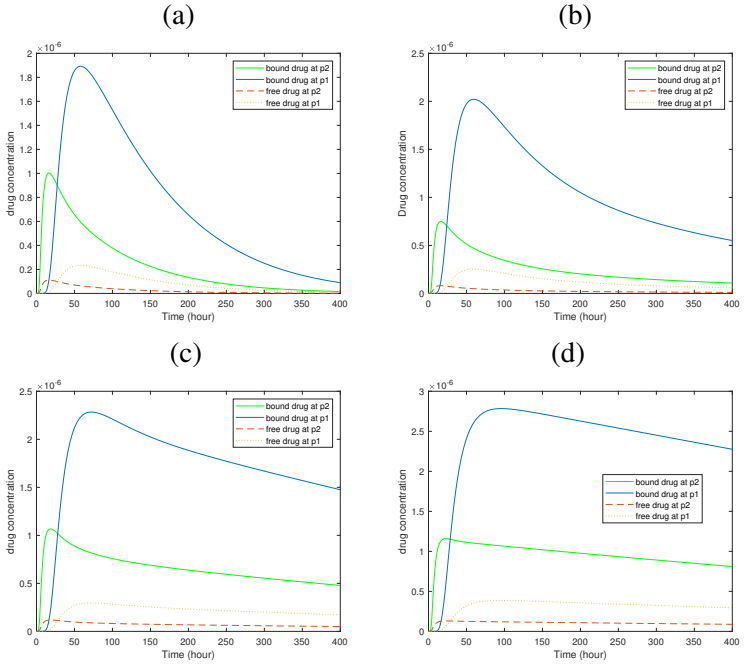

Figure 4: Temporal variation of drug concentrations at points p_1 and p_2 after 400h in high drug loading, where (a) $\frac{C_L}{C_s} = 1$, (b) $\frac{C_L}{C_s} = 2$, (c) $\frac{C_L}{C_s} = 5$ and (d) $\frac{C_L}{C_s} = 10$.

The arterial wall distribution of free and bound drug concentration can be visualized through Fig. 5. These figures show the impact of initial drug loading on the transport and distribution of drug in the arterial wall.

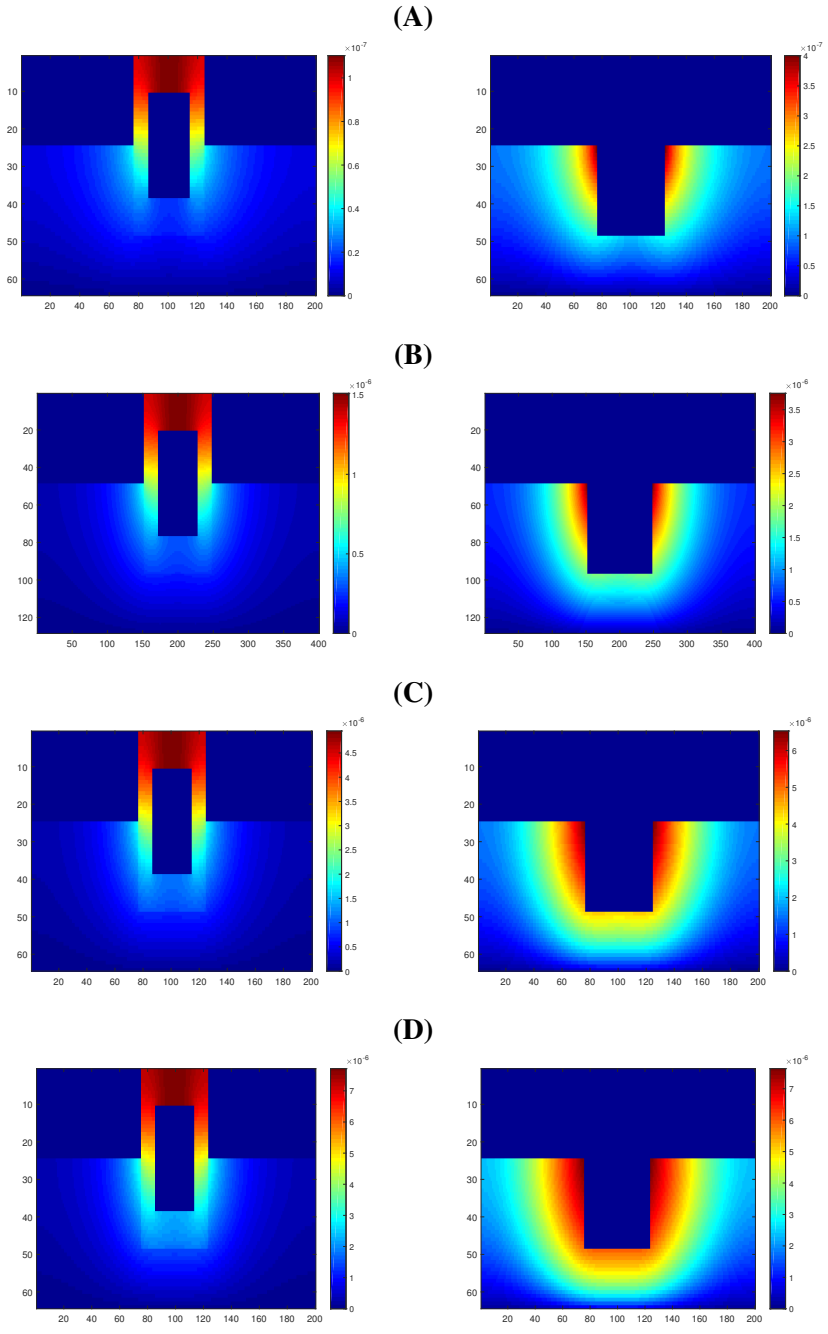

Figure 5: Drug distribution profiles for free and bound drug with different initial drug loading after 400h, where (A) $\frac{C_L}{C_s} = 1$, (B) $\frac{C_L}{C_s} = 2$, (C) $\frac{C_L}{C_s} = 5$ and (D) $\frac{C_L}{C_s} = 10$.

5.2 Impact of dissolution rate constant, k_c

In this section, we investigate the effect of dissolution rate constant on the drug release in the stent coating and the drug delivery into the arterial wall. Different values for k_c are examined to look at its impact on the drug delivery process.

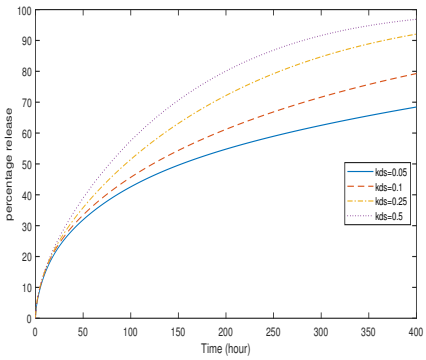

Figure 6: Drug release profiles in the stent coating at different dissolution rate constant, k_c.

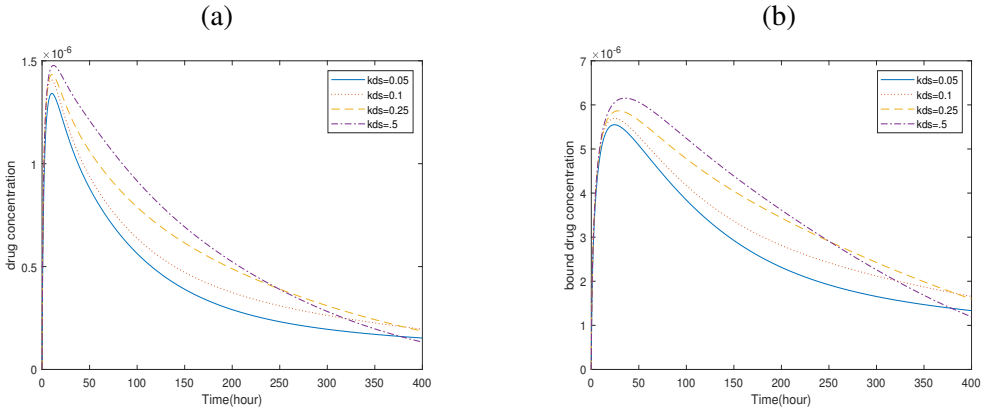

Figure 7: Temporal variation for the spatial average of (a) free and (b) bound drug concentrations in the arterial wall for different *kds*.

Fig. 6 represents with increasing k_c, the release profile can be significantly accelerate as diffusion becomes slower than dissolution kinetics. It is noteworthy that with increasing k_c the profile remains first-order. Fig. 7 represents the temporal variation for the spatial average of free and bound drug concentration in the arterial wall. while increasing k_c leads to the increasing amount of distribution of drug, but Varying k_c has little effect on average bound and free drug concentration and does not significantly affect the results. The concentrations at boundary points,P_1 and P_2, are shown in Fig. 8. As can be visualized, there are no quasi-equilibrium levels while increasing k_c and bound drug concentrations are higher than the free drug concentration at p_1. The spatial distribution of free and bound drug concentration can be visualized in Fig. 9. These simulations indicate that increasing k_c does not affect the non-uniform

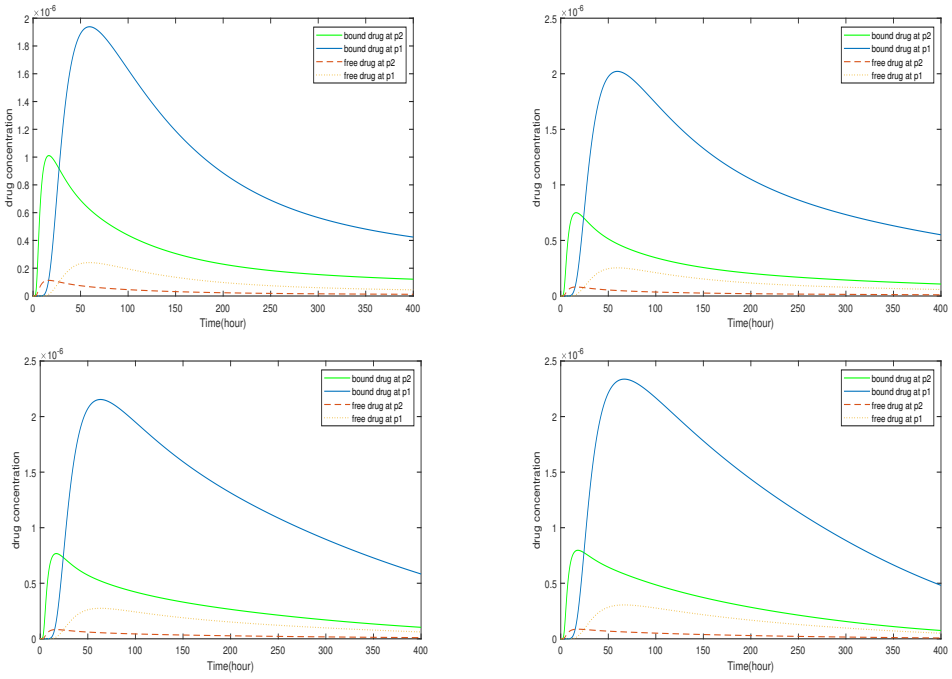

Figure 8: Temporal variation of drug concentrations at points p_1 and p_2 after 400h in high drug loading, where (a) $kds = 0.05$, (b) $kds = 0.1$, (c) $kds = 0.25$ and (d) $kds = 0.5$.

spatial distribution of drug in the arterial wall.

6 Conclusion

We have developed a mathematical model for Drug-eluting stents using a dissolution equation based on the Noyes-Withney equation combined with a function that determines the effects of dispersed drugs on dissolution processes. The model is innovative compared to the previous ones since it includes a term that is absent in diffusion-dissolution equations prior to DESs with biostable polymers.

Initially, we have presented a mathematical model for the release of a hydrophobic drug from polymer coatings and uptake by arterial walls. The presented general model has been converted to a simpler model similar to those studied in previous studies under low drug loading and into a moving boundary problem similar to those examined in the past under high drug loading and large dissolution rate limits. The numerical simulation of the nonlinear equation has been formed when the initial drug loading was higher than solubility with a finite dissolution rate.

According to simulation results, as the initial load increases, the duration of release is prolonged, zero-order profile release is derived, and the distribution of drug in the arterial wall reaches quasi-equilibrium values. While the quasi-equilibrium state was not observed in the limitation of the dissolution constant. In addition, the numerical results obtained in this numerical simulation are consistent with those found in previous studies.

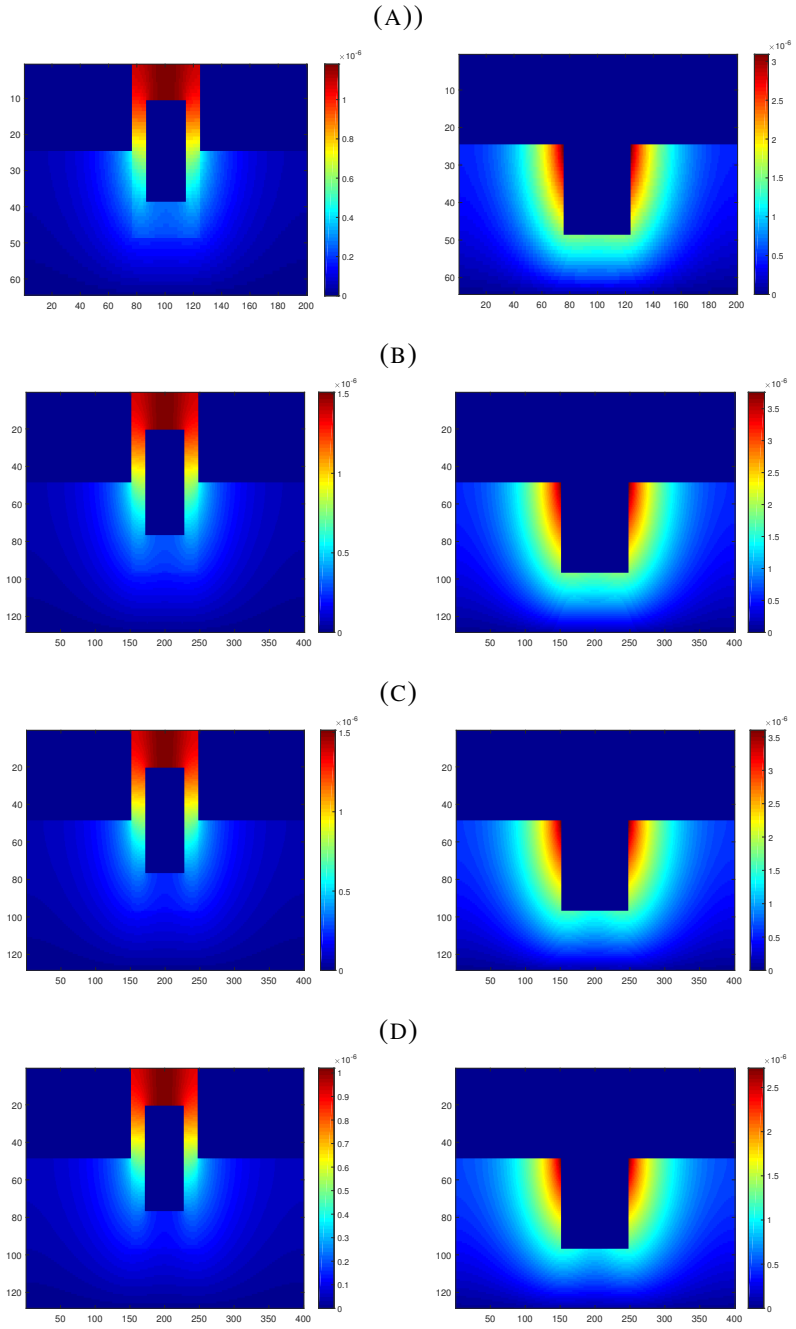

Figure 9: Drug distribution profiles for free and bound drug at different dissolution rate constant, k_c, where (A) $k_c = 0.05$, (B) $k_c = 0.1$, (C) $k_c = 0.25$ and (D) $k_c = 0.5$.

References

[1] S.R. Bailey, *Theoretical advantages and disadvantages of stent strut materials, design, thickness and surface characteristics*, J. Interv. Cardiol. **22** (2009) S3–S17.

[2] B. Balakrishnan, A.R. Tzafriri, P. Seifert, A. Groothuis, C. Rogers, E.R. Edelman, *Strut position, blood flow, and drug deposition: implications for single and overlapping drug eluting stents*, Circulation **111** (2005) 2958-2965.

[3] B. Balakrishnan, J. Dooley, G. Kopia, E.R. Edelman, *Thrombus causes fluctuations in arterial drug delivery from intravascular stents*, J. Control Release. **131** (2008) 173-180.

[4] F. Bozsak, D. Gonzalez-Rodriguez, Z. Sternberger, P. Belitz, T. Bewley, J.M. Chomaz, A.I. Barakat, *Optimization of drug delivery by drug-rluting stents*, PLoS One **10** (2015) 1–29.

[5] R.D. Braatz, X. Zhu, *Modeling and analysis of drug-eluting stents with biodegradable PLGA coating: consequences on intravascular drug delivery*, J. Biomech. Eng. **136** (2015), 111004-1–111004-10.

[6] K. Chakravarty, D.C. Dalal, *A two-phase model of drug release from microparticle with combined effects of solubilisation and recrystallisation*, Math Biosci. **272** (2016) 24-33 .

[7] K. Chakravarty, D.C. Dalal, *A nonlinear mathematical model of drug delivery from polymeric matrix*, J. Math. Biol. **81** (2019) 105-130.

[8] P. Darvishi, S. M. Salehi, *A three-dimensional mathematical model for drug delivery from drug-eluting stents*, IJCCE. **12** (2015) 15–27.

[9] M. C. Delfour, A. Garon, V. Longo, *Modeling and design of coated stents to optimize the effect of the dose*, SIAM J. Appl. Math. **65** (2005) 858-881.

[10] F. De Monte, G. Pontrelli, S. Becker, *Drug release in biological tissues*, in: S.M. Becker, A.V. Kuznetsov (Eds.), Transport in Biological Media, Elsevier Science BV, Amsterdam, 2013.

[11] L. Formaggia, S. Minisini, P. Zunino, *Modeling polymeric controlled drug release and transport phenomena in the arterial tissue*, Math. Models Methods Appl. Sci . **20** (2010) 1759-1786.

[12] G. Frenning, *Theoretical investigation of drug release from planar matrix systems: effects of a finite dissolution rate*, J. Control Release **92** (2003), 331-339.

[13] K. Gudnason, S. Sigurdssona, B. S. Snorradottirb, M. Massonb, F. Jonsdottira, *A numerical framework for drug transport in a multi-layer system with discontinuous interlayer condition*, Math. Biosci. **295** (2017) 11–23.

[14] C.W. Hwang, D. Wu, E.R. Edelman, *Physiological transport forces govern drug distribution for stent-based delivery*, J. Circulation. **104** (2001) 600-605.

[15] D.R. Hose, A.J. Narracott, B. Griffiths, S. Mahmood, J. Gunn, D. Sweeney, *A thermal analogy for modelling drug elution from cardiovascular stents*, Comput. Methods Biomech. Biomed. Engin. **7** (2004) 257-264.

[16] S. Hossainy, S. Prabhu, *A mathematical model for predicting drug release from a biodurable drug-eluting stent coating*, J. Biomed Mater. Res. A. **87** (2008) 487-493.

[17] A.J. Lee, J.R. Kingt, S. Hibberd, *Mathematical modelling of the release of drug from porous, non-swelling transdermal drug-delivery devices*, IMA J. Math. Appl. Med. Biol. **15** (1998) 135–163.

[18] N. Li, J. Steiner, S. Tang, *Convergence and stability analysis of an explicit finite difference method for 2-dimensional reactiondiffusion equations*, J Aust. Math. Soc. Ser. B **36** (1994), 234-241.

[19] A.P. Mandal, P.K. Mandal, *Computational Modelling of Three-phase Stent-based Delivery*, JERP. **2** (2017) 31–40.

[20] S. McGinty, S. McKee, R.M. Wadsworth, C. McCormick, *Modelling drug-eluting stents*, Math. Med. Biol. **28** (2011) 1-29.

[21] S. McGinty, *A decade of modelling drug release from arterial stents*, Math. Biosci. **257** (2014) 80–90.

[22] S. McGinty, S. McKee, *Release mechanism and parameter estimation in drug-eluting stent systems: analytical solutions of drug release and tissue transport*, Math Med. Biol. Math. Med. Biol. **32** (2015) 163–86.

[23] R. Mongrain, I. Faik, R.L. Leask, J. Rodes-Cabau, E. Larose, *Bertrand OF, Effects of diffusion coefficients and struts apposition using numerical simulations for drug eluting coronary stents*, J. Biomech. Eng. **129** (2007) 733-742.

[24] F. Moukalled, L. Mangani, M. Darwish, *The Finite Volume Method in Computational Fluid Dynamics*, **817**. Springer International Publishing Switzerland, 2016.

[25] G. Pontrelli, F. De Monte, *Modeling of mass dynamics in arterial drug-eluting stents*, J. Porous Media. **12** (2009) 19-28.

[26] G. Pontrelli, F. De Monte, *A multi-layer porous wall model for coronary drug eluting stents*, Int. J. Heat Mass Transf. **53** (2010) 3629-3637.

[27] P. Ravikumar, E. Bharathiraja, V. Tharani, R. Yamuna, T. Yamunarani, *Design and analysis of coronary stent*, Int. J. Healthc. Manag. **12** (2011) 447-456.

[28] R. Richtmeyer, K.W. Morton, *Difference Methods for Initial Value Problems*, Wiley, New York, 1967.

[29] I. Rykowska, I. Nowak, R. Nowak, *Drug-Eluting Stents and BalloonsMaterials, Structure Designs, and Coating Techniques: A Review*, Int. J. Mol. Sci. **25** (2020) 1-52.

[30] Sarifuddin, S. Roy, P.K. Mandal, *Computational model of stent-based delivery from a half-embedded two-layered coating*, Comput Methods Biomech Biomed Engin. **23** (2020) 815–831.

[31] J. Siepmann, F. Siepmann, *Mathematical modelling of drug delivery*, Int. J. Pharm. **364** (2008) 328-343.

[32] G.D. Smith, *Numerical Solution of Partial Differential Equations: Finite Difference Methods* (3rd ed.), Clarendon Press; Oxford University Press, Oxford, New York (1985), p. 337.

[33] H. Takebayashi, G.S. Mintz, S.G. Carlier, Y. Kobayashi, K. Fujii, T. Yasuda, R. A. Costa, I. Moussa, G. D. Dangas, R. Mehran, A.J. Lansky , E. Kreps, M.B. Collins, A. Colombo, G.W. Stone, M.B. Leon, J.W. Moses, *Nonuniform strut distribution correlates with more neointimal hyper plasia After Sirolimus-Eluting Stent Implantation*, J. Am. Heart Assoc. **110** (2004) 34303434.

[34] A.R. Tzafriri, A.D. Levin, E.R. Edelman, *Diffusion-limited binding explains binary dose response for local arterial and tumour drug delivery*, J. Cell Prolif. **42** (2009) 348-363.

[35] A.R. Tzafriri, N. Vukmirovic, V.B. Kolachalama, I. Astafieva, E.R. Edelman, *Lesion complexity determines arterial drug distribution after local drug delivery*, J. Control Release **142** (2010) 332-338.

[36] A. Tzafriri, A. Groothuis, G.S. Price, E. Edelman , *Stent elution rate determines drug deposition and receptor-mediated effects*, J. Control Release, **161** (2012) 918-926.

[37] X. Zhua, D.W. Pack, R. Braatz, *Modelling intravascular delivery from drug-eluting stents with biodurable coating: investigation of anisotropic vascular drug diffusivity and arterial drug distribution*, Computer Methods Biomech. Biomed. Engin. **17** (2014) 187–98.

[38] P. Zunino, *Multidimensional pharmacokinetic models applied to the design of drug-eluting stents*, Cardiovasc. Eng. Int. J. **4** (2004) 181-191.